Carcinoma-Associated Fibroblast–Like Differentiation of Human Mesenchymal Stem Cells

Pravin J. Mishra,[1] Prasun J. Mishra,[1,2] Rita Humeniuk,[1,2] Daniel J. Medina,[1] Gabriela Alexe,[4] Jill P. Mesirov,[4] Sridhar Ganesan,[1,2] John W. Glod,[2,3] and Debabrata Banerjee[1,2]

Departments of [1]Medicine, [2]Pharmacology, and [3]Pediatric Oncology, The Cancer Institute of New Jersey, Robert Wood Johnson Medical School, University of Medicine and Dentistry of New Jersey, New Brunswick, New Jersey and [4]The Broad Institute of Massachusetts Institute of Technology and Harvard University, Cambridge, Massachusetts

Abstract

Carcinoma-associated fibroblasts (CAF) have recently been implicated in important aspects of epithelial solid tumor biology, such as neoplastic progression, tumor growth, angiogenesis, and metastasis. However, neither the source of CAFs nor the differences between CAFs and fibroblasts from nonneoplastic tissue have been well defined. In this study, we show that human bone marrow–derived mesenchymal stem cells (hMSCs) exposed to tumor-conditioned medium (TCM) over a prolonged period of time assume a CAF-like myofibroblastic phenotype. More importantly, these cells exhibit functional properties of CAFs, including sustained expression of stromal-derived factor-1 (SDF-1) and the ability to promote tumor cell growth both *in vitro* and in an *in vivo* coimplantation model, and expression of myofibroblast markers, including α-smooth muscle actin and fibroblast surface protein. hMSCs induced to differentiate to a myofibroblast-like phenotype using 5-azacytidine do not promote tumor cell growth as efficiently as hMSCs cultured in TCM nor do they show increased SDF-1 expression. Furthermore, gene expression profiling revealed similarities between TCM-exposed hMSCs and CAFs. Taken together, these data suggest that hMSCs are a source of CAFs and can be used in the modeling of tumor-stroma interactions. To our knowledge, this is the first report showing that hMSCs become activated and resemble carcinoma-associated myofibroblasts on prolonged exposure to conditioned medium from MDAMB231 human breast cancer cells. [Cancer Res 2008;68(11):4331–9]

Introduction

Accumulating evidence suggests that tumor-associated fibroblasts or carcinoma-associated fibroblasts (CAFs) play an important role in the growth of epithelial solid tumors. It has long been known that a significant fraction of the stroma in some breast cancers consists of fibroblasts (1–3). More recent studies show that breast CAFs promote tumor cell growth compared with fibroblasts obtained from nonneoplastic locations. In addition to tumor growth, the tumor stroma has also been implicated in other important processes, such as neoplastic progression, angiogenesis, and metastasis. Whereas the potential importance of CAFs is becoming clear, the differences between tumor fibroblasts and fibroblasts from nonneoplastic tissue are not well described. Orimo and colleagues (4) defined several important characteristics of breast CAFs, including promotion of breast carcinoma cell growth, promotion of angiogenesis, and expression of myofibroblast traits. Expression of the chemokine stromal-derived factor-1 (SDF-1) has also been shown to be important in the interaction between tumor cells and stromal fibroblasts (4). Although the cell type of origin of myofibroblasts has not been conclusively established, it has been shown that they are bone marrow derived (5–10). Data from animal models as well as human breast cancers suggest that at least a subset of tumor-associated myofibroblasts is derived from circulating bone marrow cells (5–9, 11). Bone marrow origin of tumor-associated fibroblasts gains further support from the observations in an enhanced green fluorescent protein (EGFP) transplant model showing that two prominent populations of $EGFP^+$ cells were found in the tumor stroma (12). The first was determined to be fibroblasts within the tumor stromal capsule, a subset of which expressed type I collagen mRNA and α-smooth muscle actin (α-SMA). The second population was a perivascular cell associated with the $CD31^+$ tumor blood vessels. These findings suggested that some tumor-associated fibroblasts are derived from hematopoietic precursor/stem cells from the bone marrow. An attractive candidate for the bone marrow precursor of tumor-associated fibroblast is the mesenchymal stem cell (MSC).

Two features of human bone marrow–derived MSCs (hMSC) suggest that they may be the precursors of the myofibroblasts found in the tumor stroma: (*a*) MSCs develop characteristics of myofibroblasts, such as expression of α-SMA, under defined tissue culture conditions (13); (*b*) MSCs isolated from the bone marrow and labeled *ex vivo* localize to solid tumors after i.v. administration in animal models (8, 14, 15). During embryonic and fetal development, MSCs circulate in the bloodstream to seed emerging sites of hematopoiesis. They are present in large numbers in human blood for the first 12 weeks of gestation and circulating MSCs, albeit in low numbers, exist in the adult (16, 17). A recent report suggests that circulating fibrocytes derived from bone marrow precursors are the cells of origin of myofibroblasts found at wound healing sites (10). Moreover, MSCs undergo myofibroblast differentiation, including increased production of α-SMA in response to transforming growth factor-β (TGF-β), a growth factor commonly secreted by tumor cells to evade immune surveillance (18). These findings suggest that some tumor-associated fibroblasts are derived from hematopoietic precursor/stem cells derived from

Note: Supplementary data for this article are available at Cancer Research Online (http://cancerres.aacrjournals.org/).

Pravin J. Mishra and Prasun J. Mishra contributed equally to this work.

Current address for Prasun J. Mishra: Laboratory of Cancer Biology and Genetics, National Cancer Institute, NIH, Bethesda, MD 20892-4264. Current address for R. Humeniuk: Laboratory of Cellular Oncology, National Cancer Institute, NIH, Bethesda, MD 20892-4264.

Requests for reprints: Debabrata Banerjee, Department of Medicine and Pharmacology, The Cancer Institute of New Jersey, Robert Wood Johnson Medical School, University of Medicine and Dentistry of New Jersey, 195 Little Albany Street, New Brunswick, NJ 08903. Phone: 732-235-6458; Fax: 732-235-8181; E-mail: banerjed@umdnj.edu.

doi:10.1158/0008-5472.CAN-08-0943

the bone marrow. Hence, hMSCs are an attractive candidate for the bone marrow precursor of CAF.

In this study, we tested the effect of prolonged exposure (30 days) to factors in conditioned medium produced by a human breast cancer cell line MDAMB231 on the phenotype of hMSCs. Our results show that hMSCs become activated on prolonged exposure to conditioned medium from tumor cells. They exhibit myofibroblast differentiation characterized by higher expression of α-SMA, vimentin, and fibroblast surface protein (FSP) and sustained expression of SDF-1. Unlike 5-azacytidine (5-aza) treatment, hMSCs differentiated by exposure to conditioned medium show sustained expression of SDF-1 and can better support growth of MDAMB231 cells *in vitro* and in tumor xenografts in nude mice. We suggest that hMSCs are induced by tumor-derived factors to differentiate into CAFs and become part of the tumor microenvironment.

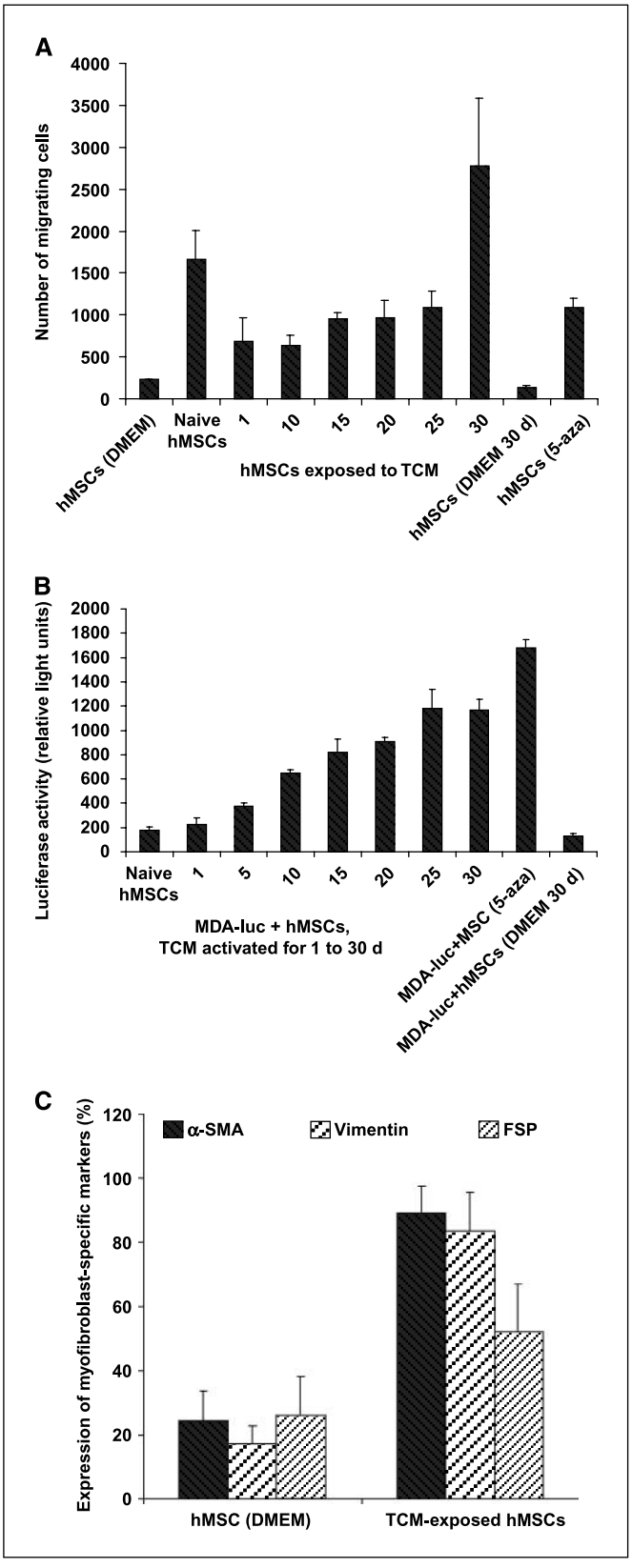

Materials and Methods

Isolation and culture of hMSCs. Unprocessed bone marrow (36×10^6 cells/mL) was purchased from Cambrex Bio Sciences Walkersville, Inc. A Ficoll gradient was used for isolation of hMSCs and to eliminate unwanted cell types from bone marrow. Cells were then plated in T75 cm^2 and six-well plate with MesenCult medium containing hMSC stimulatory supplements and fetal bovine serum (FBS) for hMSCs or α-MEM containing 10% FBS and penicillin-streptomycin. The cultures were incubated at 37°C in a humidified atmosphere containing 5% CO_2. Cells were demipopulated after 24 h and the medium was changed every other day. Cells were subcultured every 4 to 5 d and aliquots from passages 2 to 5 were frozen in liquid nitrogen for future use. Cell surface markers expressed on these cells were determined by flow cytometry using FITC-labeled antibodies (BD Biosciences) and include Stro1, CD105, CD90, HLA-ABC, and CD44, whereas they were negative for CD45, HLA-DR, and CD11b (data not shown).

Multilineage differentiation. Expanded cultures of hMSCs were analyzed for myogenic, osteogenic, and adipogenic differentiation *in vitro* to determine multipotency according to standard conditions as described before (19–23).

Tumor cell lines. Cancer cell lines MDAMB231 (American Type Culture Collection) PANC-1, and U87 were cultured in DMEM (Life Technologies) supplemented with 10% FBS and penicillin-streptomycin at 37°C in 5% CO_2.

Exposure of hMSCs to TCM. MDAMB231, PANC-1, and U87 cells were grown in DMEM + 10% heat-inactivated FBS culture medium and conditioned medium from these tumor cells was harvested after 16 h and centrifuged at 3,000 rpm for 5 min and supernatant was passed through Millipore sterile 50 mL filtration system with 0.45-μm polyvinylidene difluoride membrane. hMSCs were exposed to fresh tumor-conditioned medium (TCM) repeatedly and the TCM was changed every third day for the entire 30-d time period.

Migration assay. The migration assay was carried out as described previously (24). Briefly, Falcon tissue culture plates with 24 wells along with

Figure 1. Thirty-day TCM-exposed hMSCs migrate toward and support the growth of tumor cells and express markers for myofibroblast lineage. *A,* increased number of 30-d TCM-exposed hMSCs migrating toward the MDAMB231 cells placed at the bottom of the Transwell chamber compared with naive MSCs or the 5-aza–treated cells. Interestingly, hMSCs exposed to TCM for periods up to 25 d did not show an increase in number of migrating cells compared with the number of migrating naive hMSCs. Migration of 30-d TCM-exposed cells was significantly increased compared with naive hMSCs ($P = 0.003$) as well as with all other cell types ($P < 0.005$). *B,* increase in luciferase activity reflects growth of MDA-luc cells in a mixed culture assay. Luciferase activity was measured to determine growth of MDA-luc cells in the coculture assay. 5-Aza–treated hMSCs promote growth of MDAMB231 human breast cancer cells *in vitro* compared with naive hMSCs. One- and 5-d TCM-exposed hMSCs do not increase growth of MDAMB231 cells. A significant increase is observed with day 10 to day 20 TCM hMSCs and an additional increase is seen with day 25 and day 30 TCM-exposed hMSCs. *C,* the quantitative expression of myofibroblast marker proteins α-SMA, FSP, and vimentin in naive hMSCs and 30-d breast cancer TCM-activated hMSCs was analyzed by immunofluorescence staining (see Materials and Methods for details).

a companion Falcon cell culture inserts were used for the migration assay. Conditioned medium from tumor cells (collected after overnight culture in fresh growth medium) or tumor cells (1×10^4) were plated in the bottom chamber and incubated overnight at 37°C in 5% CO_2. Next day, the insert was placed aseptically in the well with flanges resting in the notches on the top edge of each well. Naive hMSCs or activated hMSCs (2×10^4) were plated on the top. The assay was terminated and hMSCs that had migrated through the membrane (8-μm pore size) were then stained (after removal of cells remaining on top with a wet Q-tip) using crystal violet prepared with methanol and formaldehyde.

Coculture assay *in vitro*. Luciferase-expressing MDAMB231 cells (MDA-luc; 50,000 per well) were plated in 1 mL DMEM in 12-well plates. After 24 h, hMSCs preexposed to TCM for 1 to 30 d were added (25,000 cells per well). Controls used for this assay were MDA-luc cells alone (50,000 per well) and MDA-luc cells (50,000 per well), and after 24 h, MDAMB231 (untransfected) were added as adherent cell control (25,000 per well), hMSCs were preexposed to DMEM for 30 d (25,000 per well), and hMSCs were differentiated to myogenic lineage by 5-aza (25,000 per well). After 4 d, the cells were lysed in 80 μL lysis buffer and luciferase measurements were carried out according to the manufacturer's protocol and light units were read in a luminometer.

Quantitative reverse transcription-PCR for SDF-1. SDF-1 and 18S (control) mRNA levels were examined by quantitative reverse transcription-PCR (RT-PCR). Total RNA was isolated from the cell pellets using Trizol reagent (Invitrogen). Quantitative RT-PCR was conducted using the ABI Prism 7000 Sequence Detection System (Applied Biosystems). SDF-1 mRNA levels were determined for each hMSC condition in four independent experiments and each quantitative RT-PCR was carried out in quadruplicate. Total RNA was isolated using RNeasy kit (Qiagen). A predesigned assay was used to carry out the reverse transcription (Applied Biosystems). The reaction mixture was incubated at 50°C for 30 min for reverse transcription followed by a denaturation step at 94°C for 2 min. This was followed by 35 cycles of PCR amplification at 94°C for 15 s, 55°C for 30 s, and 72°C for 1 min. The final elongation step was carried out at 72°C for 7 min. The SDF-1 primer sequences were 5′-TTTGAGAGCCATGTCGCCA-3′ (sense) and 5′-TGTCTGTTGTTGCTTTTCAGCC-3′ (antisense). Primers and probes for eukaryotic 18S rRNA, used as endogenous control, were commercially obtained (Pre-Developed Taqman Assay Reagent). Levels of SDF-1 expression are reported as a ratio ΔC_T of SDF-1 to 18S RNA. The resultant C_T value for naive hMSCs was considered to be 100% and the relative changes in levels of SDF-1 mRNA are reported as percent changes from naive hMSC levels.

Immunofluorescence analysis. The cells were plated on sterilized coverslips in 12-well plates. The cells were fixed in 4% paraformaldehyde (at room temperature, 10 min), washed with PBS, blocked with 10% FBS in a growth medium (α-MEM), and then incubated with primary antibodies for 1 h at room temperature. Cells were immunostained for α-SMA (1:250; mouse monoclonal clone 1A4, A2547), FSP (1:250; mouse monoclonal clone 1B10, F4771), and vimentin (1:200, clone VIM-13.2, V5255; Sigma-Aldrich). Secondary antibodies (1:400 in a blocking medium) used were Alexa Fluor 488P $(Ab')_2$, IgG (H+L) (Molecular Probes), and anti-mouse IgM-FITC (Sigma-Aldrich). Following further washing, the cells were counterstained with the nuclear dye TOPRO-3 iodide (1:1,000; Invitrogen, Molecular Probes) in PBS (Life Technologies) at room temperature in the dark. Cells were embedded in VectaShield mounting medium with 4′,6-diamidino-2-phenylindole (DAPI; Vector Laboratories) and examined with a fluorescence microscope. The naive and differentiated hMSCs were quantitated for the expression of myofibroblast-specific markers. Cells expressing high levels of markers with the nuclei stained with DAPI were counted in different exposures. Total cell number was obtained by counting the total number of DAPI-stained nuclei under the microscope. Percentage of marker-expressing cells to the total number of the cells was calculated.

Microarray analysis. Cells were harvested following exposure to conditioned medium and RNA was isolated using RNeasy Mini kit (Qiagen). Total RNA (5 μg) was processed for microarray analysis following verification of quality at DNA microarray core facility of The Cancer Institute of New Jersey/Robert Wood Johnson Medical School. Briefly, the RNA was reverse transcribed and hybridized to Affymetrix GeneChip Human Genome U133 Plus 2.0 array, which is composed of more than 54,000 probe sets and 1,300,000 distinct oligonucleotide features and analyzes the expression level of over 47,000 transcripts and variants, including 38,500 well-characterized human genes.

Three independent replicates for each of the experimental conditions were carried out and analyzed to control for intrasample variation. Data normalization was performed by applying the robust multiarray average method implemented in the library *affy* of the Bioconductor system.[5] Comparative analyses of expressed genes that were either down-regulated or up-regulated under various experimental conditions by >1.5-fold [permutation $P < 0.05$ and false discovery rate (FDR) < 0.25 for signal-to-noise ratio, all values expressed in log 2] were carried out using the GenePattern software available at the Broad Institute of Harvard and MIT (25).[6] Pathway analysis was performed by applying the Gene Set Enrichment Analysis software (26).[7]

Xenograft studies in nude mice. A breast cancer cell line MDAMB231 was used as a model for the study. MDAMB231 cells were injected s.c. in nude mice in five groups: (*a*) along with Matrigel (50 μL per injection; BD Biosciences) to provide extracellular environment (10×10^6 cells per mice), (*b*) along with TCM-exposed hMSCs [MDAMB231:TCM-exposed hMSCs (10×10^6:2×10^6 at a ratio of 5:1)], (*c*) along with 5-aza–treated hMSCs [MDAMB231:5-aza–treated hMSCs (10×10^6:2×10^6 at a ratio of 5:1)], (*d*) MDAMB231 cells alone (10×10^6 cells per mice), and (*e*) along with naive hMSCs [MDAMB231:naive hMSCs (10×10^6:2×10^6 at a ratio of 5:1)]. There were five animals in each of the group. All work with animals was carried out under the auspices of a protocol approved by the Institutional Animal Care and Use Committee at Robert Wood Johnson Medical School. Day of inoculation of tumors in mice was considered as day 0.

Immunohistochemistry. Tumors were excised and immediately frozen in OCT (Sakura Finetek USA, Inc.). Tissues were fixed for 24 h before processing through graded series of alcohols and embedded in paraffin wax. Thin sections (4 μm) were cut and placed onto glass slides for staining. Antigen retrieval (removing aldehyde links formed during initial fixation of tissues) was performed for over 70 min at pH 8 using EDTA. Antibody staining using 100 μL of antibody at a dilution of approximately 1:1,000 (anti-α-SMA) was applied to the slides and incubated at 37°C for 60 min. Primary antibodies were diluted with Dako-Diluent (Dako). For fibroblast marker staining, 100 μL of antibody at a dilution of 1:200 (anti-FSP) were applied to the slides and incubated at 37°C for 60 min. Tissue sections were rinsed in buffer. The diluted biotinylated secondary antibody was applied to the tissue sections and incubated for 12 min at 37°C. Hematoxylin was used as a tissue counterstain.

Statistical analysis. For statistical analysis, Student's *t* test with Benjamini FDR correction was used; $P < 0.05$ was considered significant.

Results

Effect of TCM on hMSC migration. hMSCs were either mock treated or exposed to TCM from MDAMB231 human breast cancer cells for up to 30 days and then assayed for their ability to migrate toward tumor cells in a Transwell chamber migration assay. The 30-day exposed hMSCs were found to migrate toward tumor cells in greater numbers than cells exposed to control medium or hMSCs exposed to TCM for shorter periods up to 25 days (Fig. 1*A*). Thus, prolonged exposure to secreted factors from tumor cells may "prime" hMSCs to respond to the presence of tumor cells in this assay.

Effect on tumor cell growth *in vitro*. MDAMB231-luciferase cells (hereafter MDA-luc) were grown alone or cocultured with either naive hMSCs or hMSCs exposed to TCM for 5, 10, 15, 20, or

[5] http://www.bioconductor.org
[6] http://www.broad.mit.edu/cancer/software/genepattern/
[7] http://www.broad.mit.edu/gsea/

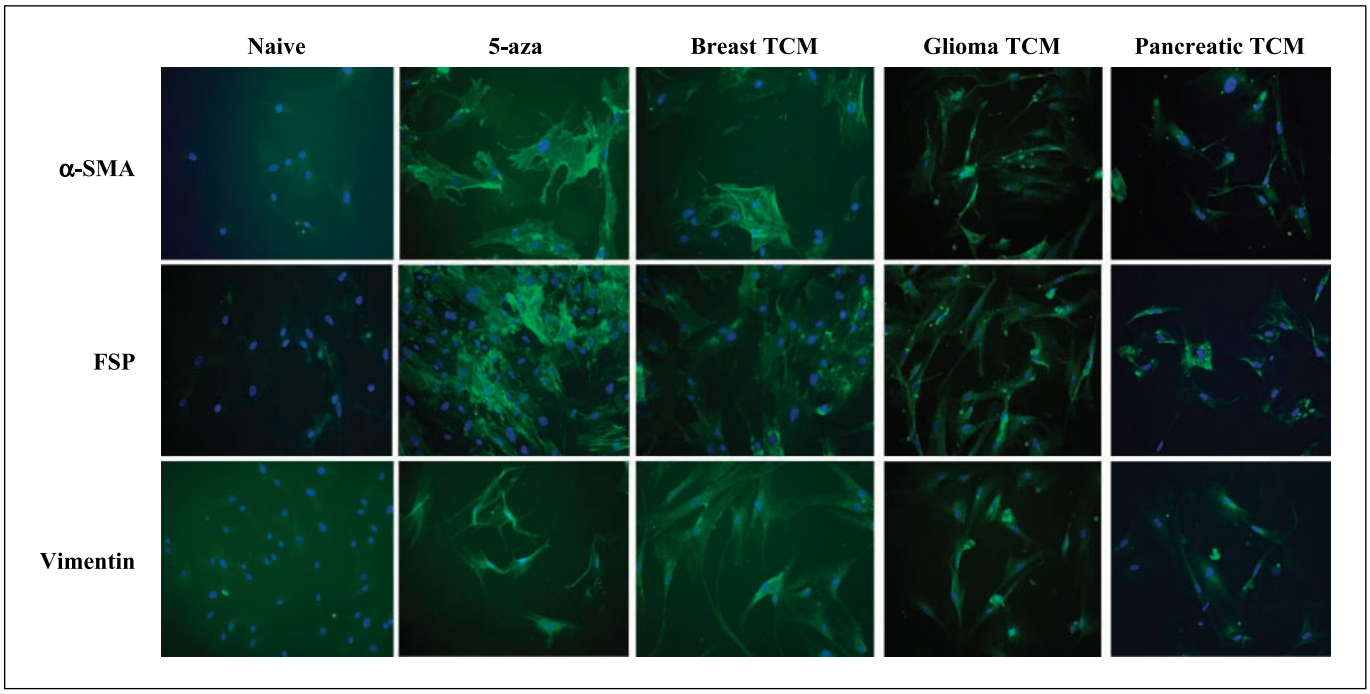

Figure 2. Increased expression of myofibroblast marker proteins α-SMA, FSP, and vimentin was observed in hMSCs exposed to TCM from breast, glioma, and pancreatic cancers and in 5-aza–treated hMSCs by immunofluorescence staining. All samples were counterstained with DAPI to visualize nuclei and appear blue in the photographs.

30 days, and tumor cell growth was assayed as described. The effect of admixed hMSCs on the growth of MDAMB231 cells was assayed. Naive hMSCs, 5-aza–treated hMSCs, or hMSCs exposed to TCM for up to 30 days were admixed with a fixed number of luciferase-expressing MDAMB231 cells. After 96 h, luciferase activity was measured as a marker of cell growth of MDAMB231 cells in these mixed cultures (Fig. 1*B*). Increasing exposure to TCM led to increasing cell growth of MDAMB231 cells by this assay. Compared with naive hMSCs, an increase in luciferase activity (growth of MDAMB231 cells) was significant for both 5-aza–treated hMSCs ($P = 0.00001$) and 30-day TCM-treated hMSCs ($P = 0.0001$), whereas there was no significant change between naive hMSCs and DMEM-exposed hMSCs ($P = 0.119$).

Activation of hMSCs by TCM from breast, glioma, and pancreatic cancers; expression of markers specific to myofibroblast lineage. Myofibroblasts can be characterized by increased expression of α-SMA, vimentin, and FSP. In addition to activation of hMSCs by TCM from MDAMB231 (representing breast cancer), we also examined the differentiation of hMSCs followed by prolonged exposure to TCM from two other types of cancers. The expression levels of α-SMA, vimentin, and FSP in activated hMSCs exposed to 30-day TCM from breast cancer (MDAMB231), glioma (U87), and pancreatic cancer cells (PANC-1) were determined by immunofluorescence. Naive hMSCs expressed little α-SMA, vimentin, and FSP, whereas hMSCs exposed to TCM for 5, 10, 15, 20, and 30 days expressed increasing amounts of α-SMA, vimentin, and FSP, indicating that the TCM-exposed hMSCs were differentiating into myofibroblasts (Fig. 2). The number of hMSCs that expressed these markers was quantitated. The analysis revealed that on average 89% of TCM-activated hMSCs expressed α-SMA, 83% expressed vimentin, and 52% expressed FSP, whereas only 17% to 26% of the naive hMSCs expressed these markers (Fig. 1*C*). Treatment with 5-aza can differentiate MSCs into myogenic lineages, which also express α-SMA, FSP, and vimentin. Indeed, the 5-aza–treated hMSCs expressed higher levels of all three proteins than the naive hMSCs (Fig. 2). Hence, we show that hMSCs exposed to TCM from three different types of cancers, breast cancer, pancreatic cancer, and glioma, differentiate and expressed markers of myofibroblast lineage (Fig. 2).

Global gene expression profiling reveals similarities between 5-aza–treated hMSCs and the 30-day TCM-exposed hMSCs. Comparison of global gene expression profiles revealed similarities between hMSCs induced to differentiate along the myogenic lineage by 5-aza–exposed and the 30-day TCM-exposed hMSCs compared with control hMSCs. Thus, 30-day TCM-exposed cells displayed similarity with cells of the myogenic lineage at the level of gene expression. The results of the global gene expression and the relationship between 5-aza–treated hMSCs and 30-day TCM-treated hMSCs are shown as unsupervised hierarchical cluster analysis in Fig. 3*A*. A similar relationship is revealed when the global gene expression profile results are presented as a dendogram as shown in Fig. 3*B*. Figure 3*C* shows a KEGG pathway analysis pie chart for genes that are up-regulated in the 30-day TCM-exposed hMSCs. Genes found to be up-regulated belong to the mitogen-activated protein kinase (MAPK) signaling, focal adhesion kinase pathway, cell cycle regulation, regulation of actin cytoskeleton pathway and cytokine-cytokine receptor interaction pathway, and the Wnt signaling pathway. Top 10 pathways enriched in genes induced by the TCM-treated hMSCs for 30 days include extracellular matrix (ECM)-receptor interaction, antigen processing and presentation, calcium signaling pathway, adherens junction, Janus-activated kinase (JAK)-signal transducer and activator of transcription (STAT) signaling pathway, Toll-like receptor signaling pathway, and TGF-β signaling pathway (Table 1).

TCM-exposed hMSCs have up-regulation of CAF-associated genes. To determine if the gene expression profile of TCM-exposed hMSCs resembled that of tumor-associated fibroblasts, we identified a set of genes that have been reported to be up-regulated in CAFs (9, 27–29). The differential expression of these reported CAF genes was then examined in the gene expression data from the TCM-exposed, 5-aza–exposed, and control-treated hMSCs. As shown in the heat map (Fig. 3*D*), TCM-exposed hMSCs did have up-regulation of a significant proportion of these CAF-associated genes. Top 25 (of 53) up-regulated genes in TCM-exposed hMSCs include *CCL2, FOS, EGR1, KRT17, CTSK, TNC, CA12, RAB3B, SESN2, HBA2, GEM, PLAU, CTHRC1, FGR, THY1, PDGFRB, FLJ23235, TCN1, COL6A1, FXYD3, NGFRAP1L1, MMP9, PDGFA*, and *COL6A2*. Top 25 (of the 47) down-regulated genes in TCM-exposed hMSCs include *ID2, CD24, MGST1, KRT19, RARRES2, KRT7, SFRP2, KRT14, MFAP4, SPINT2, CD55, C1S, KRT18, HSPA1A, BDNF, CAT, KRT8, HGF, MET, FTL, MAN2B1, JUP, PPGB*, and *TCEAL1*. These data support the notion that TCM exposure induces the differentiation of hMSCs into a state that resembles CAFs. Interestingly, a comparative study of the genes up-regulated in the 30-day TCM-exposed hMSCs and the markers for various breast cancer molecular profiles identified previously

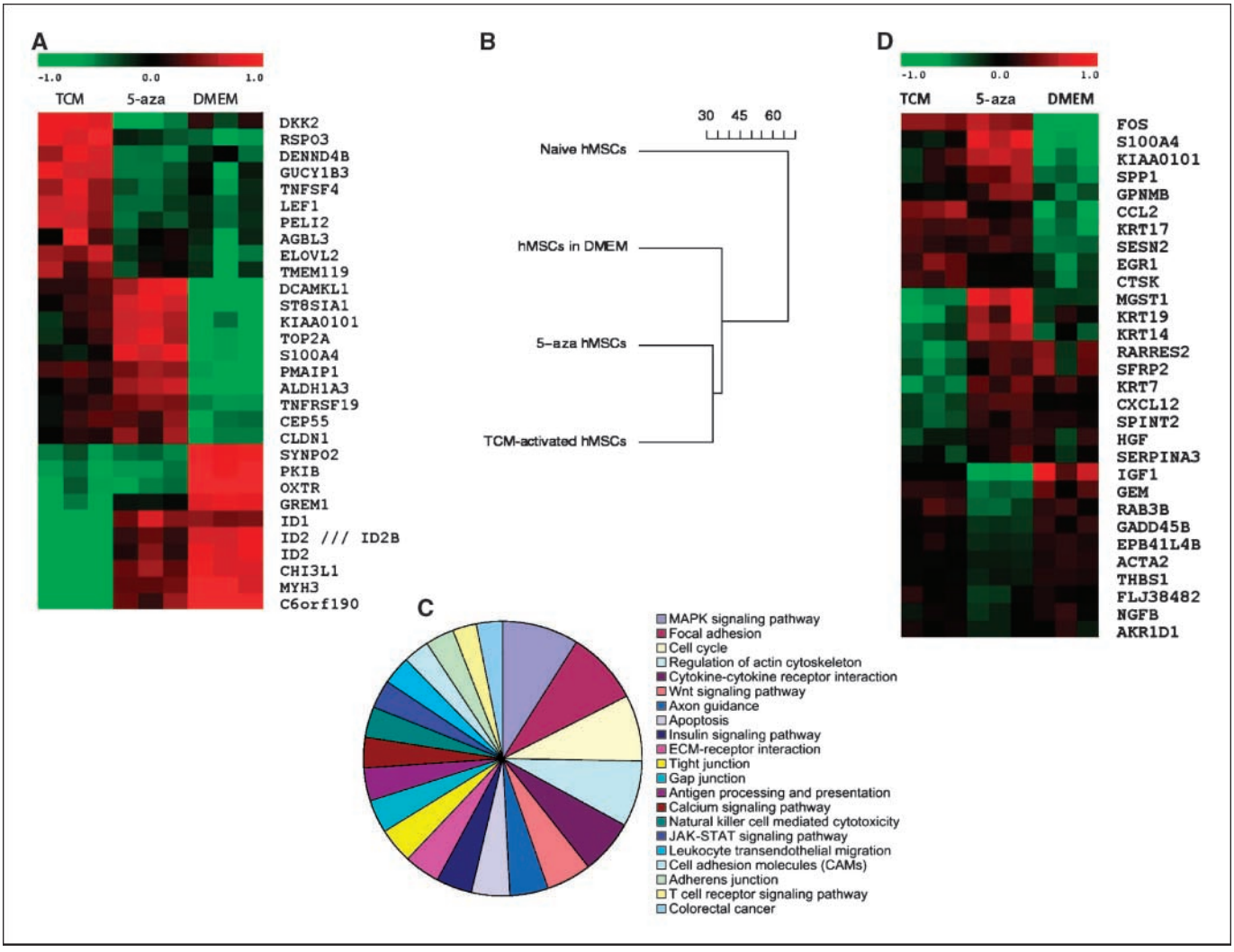

Figure 3. Comparative gene expression analysis of 30-d TCM-exposed hMSCs, 5-aza–treated hMSCs, and control DMEM-exposed hMSCs. *A,* global gene expression profile of control DMEM-exposed hMSCs, 5-aza–treated hMSCs, and 30-d TCM-exposed hMSCs. The hierarchical clustering is obtained from cDNA microarray studies carried out on naive, 5-aza–treated hMSCs, and TCM-treated hMSCs for 30 d. Overall gene expression profiles of 5-aza–treated hMSCs and 30-d TCM-exposed hMSCs is similar. Control DMEM-exposed hMSCs have a different expression profile from both 5-aza–treated as well as 30-d TCM-exposed hMSCs. The expression levels of individual transcripts are shown from green (low) to red (high). Clustering reveals an overall global gene expression profile similarity between 5-aza–treated hMSCs and 30-d TCM-exposed hMSCs compared with the control 30-d DMEM-exposed hMSCs. *Green,* lower expression; *red,* higher expression. There are several candidate genes that show increased expression in only the 30-d TCM-exposed hMSCs. *B,* dendogram depicts relative differences or similarities between the 4-h MSC samples analyzed in a hierarchical manner. The distance used for the clustering is 1-Pearson correlation between expression values (in log scale) from arrays. The 30-d TCM-exposed hMSCs seem to be closer to the 5-aza–treated cells in terms of global gene expression than the other control cell types. *C,* pie chart of induced KEGG pathways in the MSC treated by TCM for 30 d going clockwise from MAPK signaling pathway. The areas of individual slices represent percentage of genes belonging to the particular pathway that are up-regulated following activation by 30-d TCM exposure (list of genes in Table 1). *D,* gene expression array data from MSC exposed to TCM, 5-aza, or control medium were analyzed for expression of genes reported to be specifically expressed (i.e., up-regulated or down-regulated) in CAFs. A heat map showing relative expression of these genes among the three sample conditions is shown. *Red,* higher relative gene expression; *blue,* lower relative gene expression. The heat map presents 30 genes of the top 100 markers of CAF, of which 53 markers are up-regulated in TCM-exposed MSCs and 47 markers are down-regulated in TCM-exposed MSCs (see text for the gene list).

Table 1. Top 10 pathways enriched in genes induced by the TCM-treated hMSCs for 30 d

Pathways	Genes induced in the MSC treated by TCM for 30 d									
MAPK signaling pathway (P = 0.0001)	*BRAF*	*DUSP6*	*RAC1*	*CACNG6*	*TP53*	*PPP3CB*	*STMN1*	*DUSP14*	*DUSP5*	*JUND*
	JUN	*NFKB1*	*PAK2*	*IKBKB*	*MKNK2*	*CDC25B*	*NFKB2*	*RRAS2*	*CASP1*	*PDGFRB*
	PAK1	*TGFB1*	*NRAS*	*ATF4*	*HSPA8*	*MAP4K4*	*FOS*	*FGFR1*	*RASA1*	*FAS*
	MAP3K4	*HSPA9B*	*CASP7*	*CRK*	*GADD45A*	*DAXX*	*MAPK1*	*RPS6KA3*		
Focal adhesion (P = 0.0148)	*BRAF*	*RAC1*	*BIRC4*	*PPP1CC*	*TNC*	*COL6A3*	*JUN*	*CAPN2*	*SPP1*	*VASP*
	ITGA3	*PIK3R5*	*PAK2*	*COL6A1*	*ITGB3*	*BCL2*	*COL5A3*	*PPP1CA*	*TLN2*	*CCND2*
	RRAS2	*PDGFRB*	*PAK1*	*PDGFC*	*ITGB7*	*PXN*	*NRAS*	*COL6A2*	*VEGF*	*DIAPH1*
	GRLF1	*FYN*	*CRK*	*PAK3*	*ITGA7*	*LAMB1*	*ITGA2*	*ITGAV*	*MAPK1*	*IBSP*
Cell cycle (P = 0.0148)	*MCM6*	*PTTG1*	*TP53*	*CDKN1A*	*CCNB1*	*MAD2L2*	*ANAPC1*	*PCNA*	*MDM2*	*ANAPC7*
	CDC25B	*CCND2*	*CDK6*	*TGFB1*	*CCNH*	*BUB3*	*PRKDC*	*CDK4*	*YWHAQ*	*BUB1B*
	CDC23	*MCM2*	*CDC2*	*SMAD3*	*CDC16*	*GADD45A*	*CDC27*	*RBL1*	*ORC5L*	*YWHAZ*
	SMAD4	*YWHAB*	*MCM3*	*HDAC2*						
Regulation of actin cytoskeleton (P = 0.0001)	*LIMK1*	*BDKRB1*	*BDKRB2*	*BRAF*	*SSH1*	*RAC1*	*NCKAP1*	*PPP1CC*	*ITGA3*	*PIK3R5*
	ARPC5	*PFN1*	*PAK2*	*ITGB3*	*PPP1CA*	*IQGAP3*	*RRAS2*	*TIAM1*	*CFL1*	*PDGFRB*
	PAK1	*ABI2*	*ITGB7*	*PXN*	*NRAS*	*DIAPH1*	*FGFR1*	*BAIAP2*	*GRLF1*	*GSN*
	CRK	*PAK3*	*CSK*	*WASL*	*ITGA7*	*ITGA2*	*ITGAV*	*ARPC2*	*GNA13*	*MAPK1*
Cytokine-cytokine receptor interaction (P = 0.0148)	*ACVR1*	*BMPR2*	*CCL2*	*IL18R1*	*TNFSF9*	*IL6ST*	*PRLR*	*ACVR2A*	*TNFRSF12A*	*IL1RAP*
	PDGFRB	*CCL7*	*LIF*	*TGFB1*	*PDGFC*	*CLCF1*	*TNFRSF10B*	*TNFRSF10A*	*CD40*	*VEGF*
	FAS	*CSF1*	*TNFSF15*	*TNFRSF10D*	*TNFSF4*	*TNFSF18*				
Wnt signaling pathway (P = 0.0391)	*FZD9*	*FZD8*	*DAAM2*	*RAC1*	*WNT2*	*TP53*	*CSNK2A1*	*CSNK2B*	*PPP3CB*	*CSNK1A1*
	PSEN1	*NFAT5*	*WNT5A*	*JUN*	*CCND2*	*TBL1XR1*	*CSNK1E*	*FZD3*	*PLCB1*	*DKK2*
	SMAD3	*PPP2CA*	*RUVBL1*	*WNT8B*	*CACYBP*	*SMAD4*				
Axon guidance (P = 0.10337)	*LIMK1*	*CDK5*	*LRRC4C*	*RAC1*	*PLXNA2*	*PLXNA1*	*PPP3CB*	*NFAT5*	*ABLIM1*	*SEMA4F*
	PAK2	*RRAS2*	*CFL1*	*PAK1*	*NRAS*	*GNAI3*	*RASA1*	*FYN*	*PAK3*	*UNC5B*
	NRP1	*SEMA3A*	*MAPK1*							
Apoptosis (P = 0.0011)	*DFFA*	*IRAK3*	*PDCD8*	*BIRC4*	*TP53*	*RIPK1*	*CYCS*	*PPP3CB*	*CAPN2*	*PIK3R5*
	NFKB1	*IKBKB*	*BCL2*	*NFKB2*	*IL1RAP*	*TNFRSF10B*	*TNFRSF10A*	*FAS*	*CASP7*	*TNFRSF10D*
	PRKAR2A									
Insulin signaling pathway (P = 0.00116)	*PRKAG2*	*PRKAB1*	*FRAP1*	*EXOC7*	*PPP1CC*	*CALM2*	*PIK3R5*	*IKBKB*	*SOCS6*	*RPS6*
	MKNK2	*PPP1CA*	*PCK2*	*RRAS2*	*NRAS*	*CALM1*	*PKM2*	*IRS4*	*PYGB*	*IRS1*
	CRK	*EIF4EBP1*	*MAPK1*	*PRKAR2A*						
Gap junction (P = 0.0230)	*TUBB2C*	*ITPR2*	*CSNK1A1*	*ADCY3*	*RRAS2*	*PDGFRB*	*PDGFC*	*CSNK1E*	*TUBA6*	*PLCB1*
	GNAI3	*CDC2*	*GNAS*	*CSNK1G1*	*GUCY1B3*	*MAPK1*	*TUBB*			

NOTE: Each of these pathways contains >75% induced genes. Among other enriched pathways, containing between 40% and 75% induced genes: ECM-receptor interaction, antigen processing and presentation, calcium signaling pathway, adherens junction, JAK-STAT signaling pathway, Toll-like receptor signaling pathway, and TGF-β signaling pathway.

(30) revealed that 25% of the TCM-exposed hMSC markers are up-regulated in the basals, 15% are up-regulated in luminals, and <5% are up-regulated in the $HER2^+$ subtype of human breast cancers (data not shown). The markers up-regulated in TCM-activated hMSCs and down-regulated in the hMSCs treated with 5-aza and naive hMSCs grown in DMEM include genes involved in several functional classes, including transmembrane, signal transduction, and splicing. Markers up-regulated in 5-aza–treated cell lines include several genes involved in DNA metabolism and cellular processes. Markers up-regulated in naive hMSCs grown in DMEM include genes involved in glycoprotein and binding processes and in cellular metabolism (see information of the gene list in Supplementary Data S1).

Sustained expression of SDF-1 in 30-day TCM-treated hMSCs. One critical feature of CAFs identified is their ability to secrete SDF-1, which may support tumor cell growth (4). We determined the effect of TCM exposure on SDF-1 expression in hMSCs. Real-time quantitative PCR analysis revealed a sustained high level of SDF-1 gene expression in hMSCs treated for 30 days in TCM compared with naive hMSCs (P = 0.032). The increase in SDF-1 mRNA level was 2-fold compared with the DMEM control (Fig. 4*A*). In contrast, the 5-aza–treated hMSCs did not show

increased expression of SDF-1 compared with the naive hMSCs ($P = 0.12$). The mRNA levels of SDF-1 were normalized to 18S RNA that was used as a control for the RT-PCR amplification.

Activated hMSCs promote tumor growth *in vivo*. To determine if 30-day TCM-exposed hMSCs can support tumor growth *in vivo*, a set of xenograft experiments was performed using MDAMB231 human breast cancer cells. The MDAMB231 cells do not form tumors in nude mice when injected alone; however, robust tumor growth can be induced when they are mixed with Matrigel before injection (31). To determine the effect of hMSCs on tumor cell growth under these conditions, 10×10^6 MDAMB231 cells were injected into the backs of nude mice mixed with either Matrigel, naive hMSCs, 5-aza–treated hMSCs, or 30-day TCM-treated hMSCs (2×10^6 hMSCs were injected along with 10×10^6 MDAMB231 cells). Both the presence of Matrigel and 30-day TCM-treated hMSCs clearly supported tumor growth when compared with MDAMB231 alone (Fig. 4*B*). The naive hMSCs and the 5-aza–treated hMSCs did not seem to support tumor growth as robustly as either Matrigel or 30-day TCM-treated hMSCs. The naive as well as the 30-day TCM hMSCs did not form tumors when injected s.c. in nude mice.

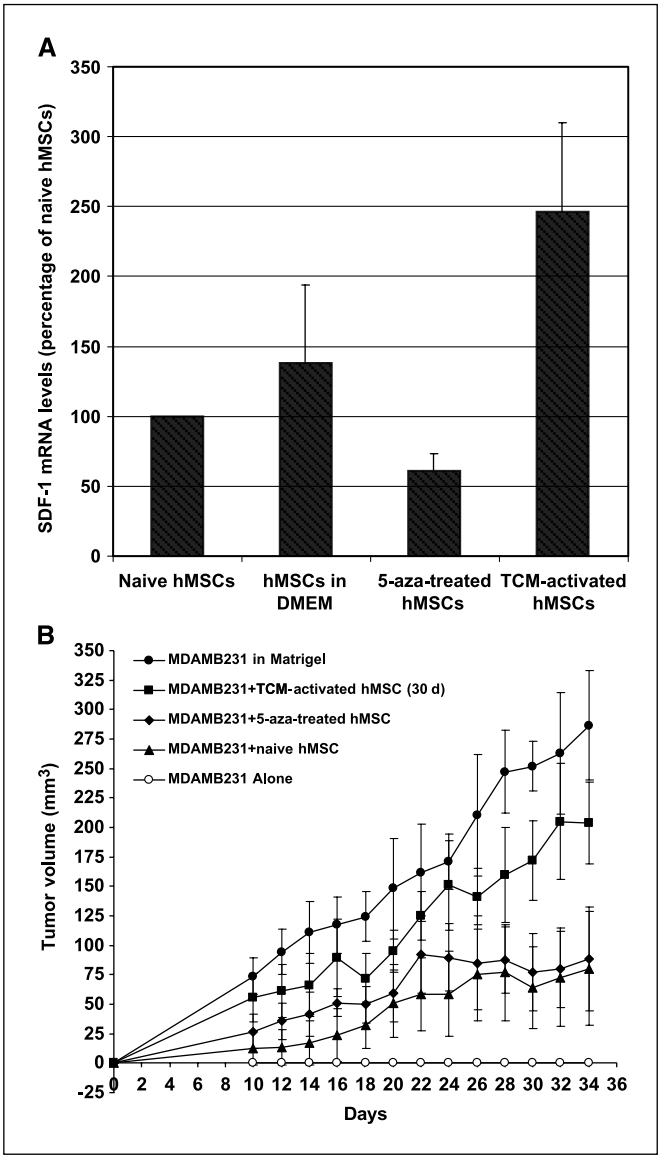

Figure 4. TCM-activated hMSCs have increased expression of SDF-1 and promote breast tumor growth in nude mice. *A,* expression of SDF-1, a marker of myofibroblasts, is increased in 30-d TCM-exposed hMSCs. Levels of SDF-1 mRNA were quantitated by quantitative RT-PCR and expressed as fold change over 18S RNA levels. For naive MSCs, the ratio of SDF-1 over 18S RNA is taken as 100%. Changes in levels of SDF-1 mRNA/18S RNA following exposure of naive MSCs to the various conditions are reported as percent changes. *B,* 30-d TCM-exposed hMSCs when injected together with MDAMB231 cells result in robust tumor growth in nude mice. *In vivo* tumor growth was measured over 24 d in nude mice ($n = 5$ for all groups). MDAMB231 cells along with or without TCM-exposed hMSCs, naive hMSCs, 5-aza–treated hMSCs, or Matrigel were injected and palpable tumors were seen on day 10 (tumor cells injected on day 0). The human breast cancer cells MDAMB231 when injected alone did not form tumors in nude mice as shown. Matrigel as well as 30-d TCM-exposed hMSCs increase growth of MDAMB231 tumors in nude mice compared with naive hMSCs and 5-aza–treated hMSCs. The naive hMSCs and the 5-aza–treated hMSCs did not show the same robust tumor formation as seen for Matrigel and 30-d TCM-exposed hMSC group. *Y axis,* tumor volume; *X axis,* days following tumor cell injection. *Points,* mean; *bars,* SD.

hMSC-derived cells expressing myofibroblast markers contribute to stroma of mixed xenograft tumors. At the end of the observation period, tumors were excised from the animals, frozen in OCT, and processed for immunohistochemical staining for α-SMA and FSP (Fig. 5). The strongest positivity for FSP was seen in tumors derived from 30-day TCM-treated hMSCs + MDAMB231 group. The coinjected hMSCs exposed to 30-day TCM showed a similar pattern of distribution within the tumor section resembling earlier observations in endometrial cancers for CAFs (32). This suggests that the 30-day TCM-exposed hMSCs may become functionally incorporated into the tumor stroma and facilitate tumor growth to a greater extent than the other cell types when comingled with MDAMB231 human breast cancer cells.

Discussion

The surrounding tumor microenvironment seems to be an important determinant in the final outcome of the disease (32, 33). Our results show that myofibroblasts derived from hMSCs are associated with the tumor microenvironment and are a source of CAFs. Our conclusions are based on the observations that long-term exposure of MSCs to TCM from human breast cancer cells induces a phenotype that resembles the reported myofibroblast-like features in CAFs, including increased expression of SMA, FSP, and vimentin and sustained expression of SDF-1. Moreover, the 30-day TCM-exposed cells supported tumor growth *in vitro* as well as *in vivo*. Conversely, the naive hMSCs expressed little α-SMA, FSP, or vimentin and did not support robust tumor growth *in vitro* or *in vivo*. This agrees with a recent report showing that naive hMSCs can inhibit tumor growth *in vivo* in a model of Kaposi's sarcoma (34).

Additionally, gene expression profile of the 30-day TCM-exposed hMSCs resembles that of 5-aza–treated hMSCs to a great extent and is distinct from those of either the DMEM control hMSCs or the naive hMSCs. Thus, 30-day TCM-exposed hMSCs seem to be similar to cells of myogenic lineage at many levels. There are now several examples in the literature of changes in gene expression by MSCs brought about by exposure to various stimuli.

Myofibroblastic properties have also been induced in bone marrow–derived MSCs *in vitro* (13). Increased expression of α-SMA and vimentin has been noted after 14 to 21 days following exposure to fibroblast growth factor-2 as well as mechanical stress (35, 36). In addition to α-smooth muscle markers,

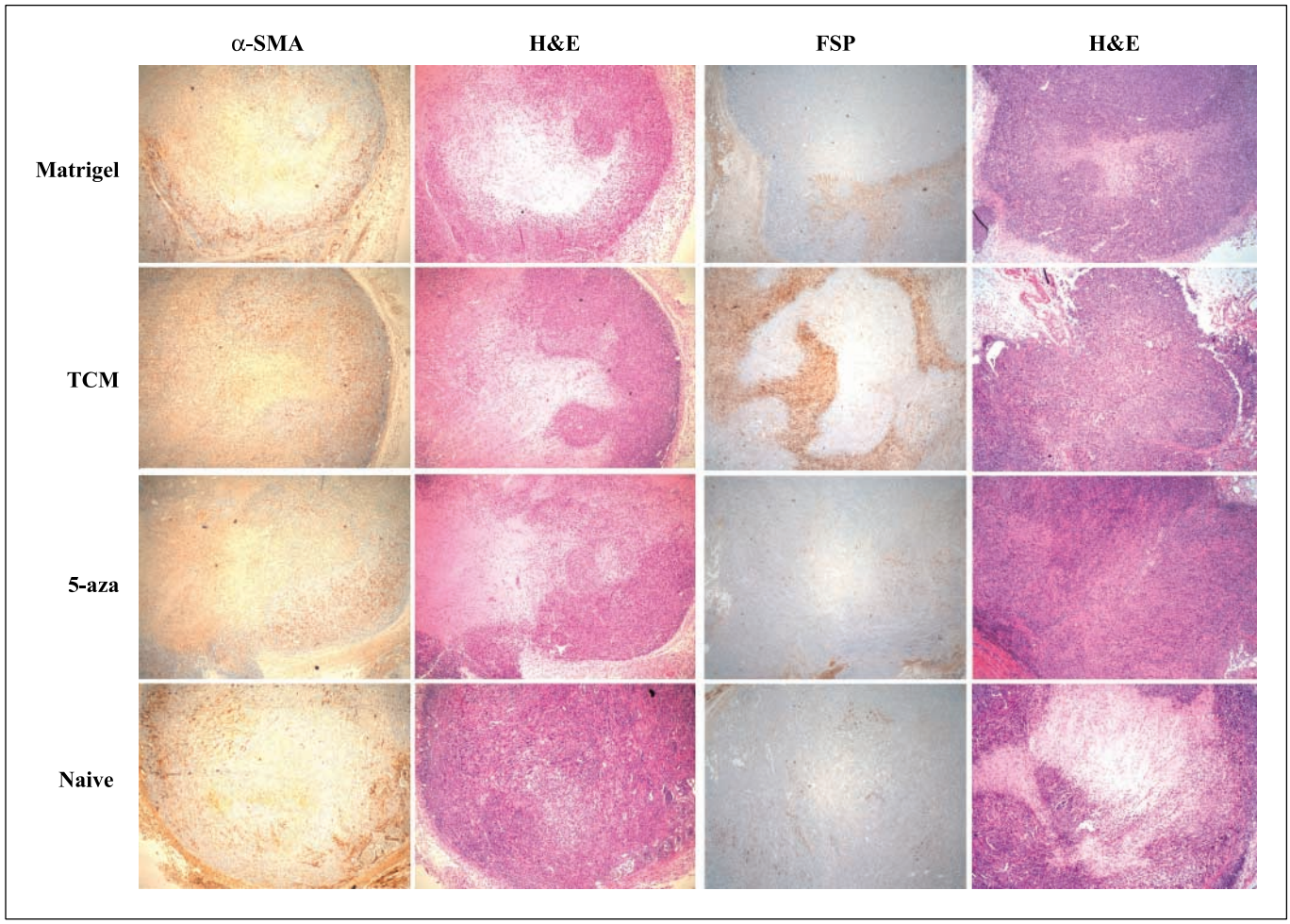

Figure 5. Thirty-day TCM-exposed hMSCs become incorporated in the tumor stroma to a greater extent than the other coinjected cell types. Immunohistochemical staining for myofibroblast markers α-SMA, FSP, and H&E stain in tumor stroma from naive hMSC + MDAMB231 tumors (small tumor that did not grow in size), MDAMB231 plus Matrigel tumors, and MDAMB231 plus 5-aza–treated hMSCs and tumors from MDAMB231 plus 30-d TCM-exposed hMSCs, respectively.

tumor-associated fibroblasts express high levels of SDF-1, which is important in promoting both tumor growth and angiogenesis (4). Although the phenotypic appearance of hMSCs differentiated to myofibroblasts using various inducers is similar, there maybe important functional differences as highlighted by our observation that 5-aza–treated hMSCs do not support robust *in vivo* tumor growth as do the 30-day TCM-exposed hMSCs. Our studies also suggest that factors secreted by tumor cells present in TCM can recruit hMSCs and influence them to become part of the tumor microenvironment.

The time taken (30 days) by hMSCs to exhibit myofibroblast-like properties presented in our study represents a combination of properties. The primary criteria were to see a clear effect on increased tumor cell growth *in vitro*, and this approximately coincided with the time taken *in vitro* for conventional differentiation assays, such as induction of differentiation into myogenic, osteogenic, adipogenic, and chondrogenic lineages for the naive hMSCs. A single criterion, such as increased expression of α-SMA, can be observed earlier (37). The increased expression of α-SMA was observed following incubation of hMSCs to conditioned medium from human colorectal cancer cells as well as TGF-β1 (37). It is possible that inclusion of recombinant TGF-β1 in addition to the TCM may have contributed to an earlier phenotypic change in the hMSCs than exposure to TCM alone. We observed a gradual increase in α-SMA levels following exposure to TCM, which is in consent with the observation that stroma formation in hMSC-transplanted tumor-bearing mice showed that expression of α-SMA increased from 25.3% to 39.8% from day 14 to day 28, indicating that the change may be progressive both qualitatively as well as quantitatively *in vivo* (5). Combined with recent studies showing that CAFs are derived from cells present in the bone marrow, that MSCs are present in the circulation, and that MSCs localize to solid tumors when administered systemically in animal models, these data provide compelling evidence that hMSCs are a source of CAFs. Although these data show the ability of hMSCs to form CAFs, they do not preclude the possibility that CAFs may arise from other sources, including epithelial-mesenchymal transition. It is possible that epithelial-mesenchymal transition may have also contributed to the stromal layer. This possibility would have to be evenly distributed among the three experimental conditions (i.e., Matrigel control, 30-day TCM-exposed MSCs, and naive MSCs) and thus would have resulted in nearly equal staining in the three cases. Although this possibility exists for epithelial tumors, it is

unlikely to contribute to the staining observed in the experimental groups presented here. It has been shown that mutations and loss of heterozygosity in the stromal compartment do not always overlap with the mutations and loss of heterozygosity in the epithelial compartment in breast cancers (38). This suggests that different pathways of clonal expansion may have been involved in tumor and stroma development.

In vitro and coimplantation models combining tumor cells and hMSCs hold great promise for providing a system in which the interaction between tumor and stroma can be manipulated and studied. Additionally, these studies provide a cell culture method for generating one of the important cell types of the tumor stroma—the activated myofibroblasts. A better understanding of the interplay between different bone marrow–derived cell types and the tumor cells within the tumor microenvironment will be important in developing strategies for improved tumor therapy that takes into account the influence of tumor microenvironment on tumor survival and growth.

Disclosure of Potential Conflicts of Interest

No potential conflicts of interest were disclosed.

Acknowledgments

Received 8/22/2007; revised 3/13/2008; accepted 3/31/2008.

Grant support: The Cancer Institute of New Jersey collaborative research grant (D. Banerjee and J.W. Glod), The New Jersey Commission on Cancer Research grant 05-2406-CCR-EO, and New Jersey Commission on Science and Technology New Jersey Stem Cell Initiative grant HESC-06-04-00.

The costs of publication of this article were defrayed in part by the payment of page charges. This article must therefore be hereby marked *advertisement* in accordance with 18 U.S.C. Section 1734 solely to indicate this fact.

The microarray data have been submitted to the GEO database and are available under the accession number GSE9764 at http://www.ncbi.nlm.nih.gov/geo/query/acc.cgi.

References

1. Bissell MJ, Radisky D. Putting tumours in context. Nat Rev Cancer 2001;1:46–54.
2. Blankenstein T. The role of tumor stroma in the interaction between tumor and immune system. Curr Opin Immunol 2005;17:180–6.
3. Cardone A, Tolino A, Zarcone R, Borruto Caracciolo G, Tartaglia E. Prognostic value of desmoplastic reaction and lymphocytic infiltration in the management of breast cancer. Panminerva Med 1997;39:174–7.
4. Orimo A, Gupta PB, Sgroi DC, et al. Stromal fibroblasts present in invasive human breast carcinomas promote tumor growth and angiogenesis through elevated SDF-1/CXCL12 secretion. Cell 2005;121:335–48.
5. Ishii G, Sangai T, Oda T, et al. Bone-marrow-derived myofibroblasts contribute to the cancer-induced stromal reaction. Biochem Biophys Res Commun 2003;309:232–40.
6. Direkze NC, Hodivala-Dilke K, Jeffery R, et al. Bone marrow contribution to tumor-associated myofibroblasts and fibroblasts. Cancer Res 2004;64:8492–5.
7. Direkze NC, Jeffery R, Hodivala-Dilke K, et al. Bone marrow-derived stromal cells express lineage-related messenger RNA species. Cancer Res 2006;66:1265–9.
8. Studeny M, Marini FC, Dembinski JL, et al. Mesenchymal stem cells: potential precursors for tumor stroma and targeted-delivery vehicles for anticancer agents. J Natl Cancer Inst 2004;96:1593–603.
9. Allinen M, Beroukhim R, Cai L, et al. Molecular characterization of the tumor microenvironment in breast cancer. Cancer Cell 2004;6:17–32.
10. Mori L, Bellini A, Stacey MA, Schmidt M, Mattoli S. Fibrocytes contribute to the myofibroblast population in wounded skin and originate from the bone marrow. Exp Cell Res 2005;304:81–90.
11. Chauhan H, Abraham A, Phillips JR, Pringle JH, Walker RA, Jones JL. There is more than one kind of myofibroblast: analysis of CD34 expression in benign, *in situ*, and invasive breast lesions. J Clin Pathol 2003;56:271–6.
12. LaRue AC, Masuya M, Ebihara Y, et al. Hematopoietic origins of fibroblasts. I. *In vivo* studies of fibroblasts associated with solid tumors. Exp Hematol 2006;34:208–18.
13. Hung SC, Kuo PY, Chang CF, Chen TH, Ho LL. α-Smooth muscle actin expression and structure integrity in chondrogenesis of human mesenchymal stem cells. Cell Tissue Res 2006;324:457–66.
14. Studeny M, Marini FC, Champlin RE, Zompetta C, Fidler IJ, Andreeff M. Bone marrow-derived mesenchymal stem cells as vehicles for interferon-β delivery into tumors. Cancer Res 2002;62:3603–8.
15. Hung SC, Deng WP, Yang WK, et al. Mesenchymal stem cell targeting of microscopic tumors and tumor stroma development monitored by noninvasive *in vivo* positron emission tomography imaging. Clin Cancer Res 2005;11:7749–56.
16. Campagnoli C, Roberts IA, Kumar S, Bennett PR, Bellantuono I, Fisk NM. Identification of mesenchymal stem/progenitor cells in human first-trimester fetal blood, liver, and bone marrow. Blood 2001;98:2396–402.
17. Kuznetsov SA, Mankani MH, Gronthos S, Satomura K, Bianco P, Robey PG. Circulating skeletal stem cells. J Cell Biol 2001;153:1133–40.
18. Wang D, Park JS, Chu JS, et al. Proteomic profiling of bone marrow mesenchymal stem cells upon transforming growth factor β1 stimulation. J Biol Chem 2004;279:43725–34.
19. Wakitani S, Saito T, Caplan AI. Myogenic cells derived from rat bone marrow mesenchymal stem cells exposed to 5-azacytidine. Muscle Nerve 1995;18:1417–26.
20. Neuhuber B, Gallo G, Howard L, Kostura L, Mackay A, Fischer I. Reevaluation of *in vitro* differentiation protocols for bone marrow stromal cells: disruption of actin cytoskeleton induces rapid morphological changes and mimics neuronal phenotype. J Neurosci Res 2004;77:192–204.
21. Friedman MS, Long MW, Hankenson KD. Osteogenic differentiation of human mesenchymal stem cells is regulated by bone morphogenetic protein-6. J Cell Biochem 2006;98:538–54.
22. Gregory CA, Prockop DJ, Spees JL. Non-hematopoietic bone marrow stem cells: molecular control of expansion and differentiation. Exp Cell Res 2005;306:330–5.
23. Pittenger MF, Mackay AM, Beck SC, et al. Multilineage potential of adult human mesenchymal stem cells. Science 1999;284:143–7.
24. Menon LG, Picinich S, Koneru R, et al. Differential gene expression associated with migration of mesenchymal stem cells to conditioned medium from tumor cells or bone marrow cells. Stem Cells 2007;25:520–8.
25. Reich M, Liefeld T, Gould J, Lerner J, Tamayo P, Mesirov JP. GenePattern 2.0. Nat Genet 2006;38:500–1.
26. Subramanian A, Tamayo P, Mootha VK, et al. Gene set enrichment analysis: a knowledge-based approach for interpreting genome-wide expression profiles. Proc Natl Acad Sci U S A 2005;102:15545–50.
27. Hu M, Yao J, Cai L, et al. Distinct epigenetic changes in the stromal cells of breast cancers. Nat Genet 2005;37:899–905.
28. Finak G, Sadekova S, Pepin F, et al. Gene expression signatures of morphologically normal breast tissue identify basal-like tumors. Breast Cancer Res 2006;8:R58.
29. Chang HY, Sneddon JB, Alizadeh AA, et al. Gene expression signature of fibroblast serum response predicts human cancer progression: similarities between tumors and wounds. PLoS Biol 2004;2:E7.
30. Wang Y, Klijn JG, Zhang Y, et al. Gene-expression profiles to predict distant metastasis of lymph-node-negative primary breast cancer. Lancet 2005;365:671–9.
31. Mehta RR, Graves JM, Hart GD, Shilkaitis A, Das Gupta TK. Growth and metastasis of human breast carcinomas with Matrigel in athymic mice. Breast Cancer Res Treat 1993;25:65–71.
32. Orimo A, Tomioka Y, Shimizu Y, et al. Cancer-associated myofibroblasts possess various factors to promote endometrial tumor progression. Clin Cancer Res 2001;7:3097–105.
33. Kaminski A, Hahne JC, Haddouti el M, Florin A, Wellmann A, Wernert N. Tumour-stroma interactions between metastatic prostate cancer cells and fibroblasts. Int J Mol Med 2006;18:941–50.
34. Khakoo AY, Pati S, Anderson SA, et al. Human mesenchymal stem cells exert potent antitumorigenic effects in a model of Kaposi's sarcoma. J Exp Med 2006;203:1235–47.
35. Hankemeier S, Keus M, Zeichen J, et al. Modulation of proliferation and differentiation of human bone marrow stromal cells by fibroblast growth factor 2: potential implications for tissue engineering of tendons and ligaments. Tissue Eng 2005;11:41–9.
36. Kobayashi N, Yasu T, Ueba H, et al. Mechanical stress promotes the expression of smooth muscle-like properties in marrow stromal cells. Exp Hematol 2004;32:1238–45.
37. Emura M, Ochiai A, Horino M, Arndt W, Kamino K, Hirohashi S. Development of myofibroblasts from human bone marrow mesenchymal stem cells cocultured with human colon carcinoma cells and TGFβ1. In Vitro Cell Dev Biol Anim 2000;36:77–80.
38. Patocs A, Zhang L, Xu Y, et al. Breast-cancer stromal cells with TP53 mutations and nodal metastases. N Engl J Med 2007;357:2543–51.